Comparative Study of Metallic and Non-metallic Stiffened Plates in Marine Structures

Jeong, Han Koo†

Abstract

In this paper, a comparative study of metallic and non-metallic stiffened plates under a lateral pressure load is performed using conventional statistically determinate and SQP(Sequential Quadratic Programming) optimisation approaches. Initially, a metallic flat-bar stiffened plate is exemplified from the superstructure of a marine vessel and, subsequently, its structural topology is varied as hat-section stiffened FRP(Fibre Reinforced Plastics) single skin plates and monocoque FRP sandwich plates having a PVC foam core. These proposed structural alternatives are analysed using elastic closed-form solutions and SQP optimisation method under stress and deflection limits obtained from practice to calculate and optimise geometry dimensions and weights. Results obtained from the comparative study provide useful information for marine designers especially at the preliminary design stage where various building materials and structural configurations are dealt with.

Keywords *: flat-bar stiffened metallic plate, hat-section stiffened FRP plate, Monocoque FRP sandwich plate, statically determinate solution, SQP optimisation solution*

1. Introduction

Stiffened plates require simple fabrication methods and have good strength to weight ratios. For these reasons, they can easily be seen in marine vessels as important secondary structural members. A conventional flat-bar stiffened metallic plate is a typical example. Its structural topology is varied as manufacturing techniques are advanced and new building materials are introduced. Non-metallic materials like FRP composites materials and environment friendly closed manufacturing techniques like VARIM (Vacuum Assisted Resin Infusion Molding) and SCRIMP (Seemann Composites Resin Infusion Molding Process) are the case in point. Naturally, these availabilities give marine designers more choices. Therefore, efficient assessment of various structural topologies is an important task for marine designers especially at the preliminary design stage where the choice of materials and the configuration of the stiffened plate can be defined before a final decision on the selection of the stiffened plate. In this assessment, the designers can rely on conventional statistically determinant and optimisation approaches rather than detailed finite element analysis. In the literature, many researches have been carried out with regard to the structural design of stiffened plates. However, they dealt with either metallic or non-metallic structure in a specified configuration and material. Early researches done in 1930's~1960's mainly dealt with the structural design of flat grillages and transversely stiffened plates for steel (Clarkson, 1965; Muckle, 1967). As marine applications built in FRP composite materials were introduced such as HMS Wilton in 1973, researches on the structural design of stiffened FRP composite plates started to expand and comprehensive elastic closed-form solutions became available (Smith, 1990). Later on, optimisation methods were introduced and incorporated into the structural design of stiffened plates (Davalos *et al.*, 1996; He *et al.*, 2003; Liu *et al.*,

† 책임저자, 정회원 · 군산대학교 조선공학과 조교수
Tel: 063-469-1853 ; Fax: 063-469-1851
E-mail: hkjeong@kunsan.ac.kr

• 이 논문에 대한 토론을 2011년 2월 28일까지 본 학회에 보내주시면 2011년 4월호에 그 결과를 게재하겠습니다.

2000; Sedaghati *et al.*, 2003). In these researches, metallic based truss and frame structures, longitudinally stiffened plates, and FRP composite based I-beams, box-beam sections, sandwich structures and stiffened plates were optimised for minimum weights, maximum load and optimal geometry dimensions/material architecture such as fibre orientations and volumes. It should be mentioned that there are a large number of research publications on this subject and the cited references are not necessarily the only significant contributions. From this literature review, it is hard to find evidence of a systematic assessment of various metallic and non-metallic stiffened plates in equivalent design for a comparative purpose, which is useful information for marine designers at the preliminary design stage. Thus in this paper, a comparative study of metallic and non-metallic stiffened plates under a lateral pressure load is performed using conventional statistically determinant and SQP optimisation approaches. A flat-bar stiffened aluminium plate is exemplified from the superstructure of a marine vessel and its alternatives are proposed as hat-section stiffened FRP plates and monocoque FRP sandwich plates having a PVC foam core. For FRP four different material properties are considered and they are high strength and ultra-high modulus CFRP, and low and high moduli GFRP. In total 9 different structural alternatives are proposed. These are analysed using elastic closed-form solutions under stress and deflection limits, as design constraints, obtained from practice: geometry dimensions and weights are calculated when the given deign constraints are satisfied. Afterwards SQP optimisation method is used in conjunction with the closed-form solutions and this is applied to the structural alternatives with a view to optimise their scantlings and minimise their weights.

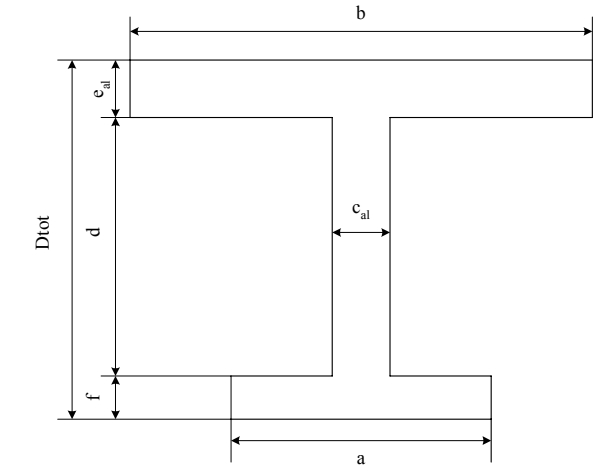

(a) Flat-bar stiffened aluminium beam model

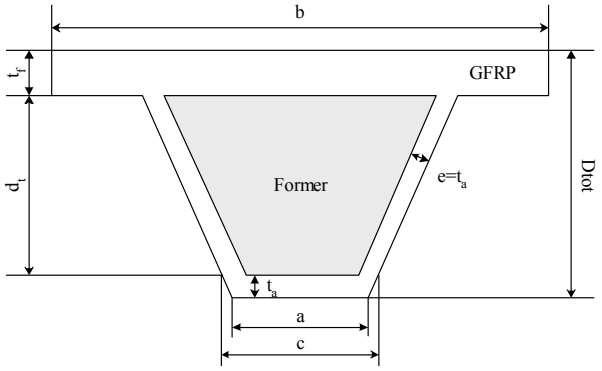

(b) Hat-section stiffened FRP single skin beam model

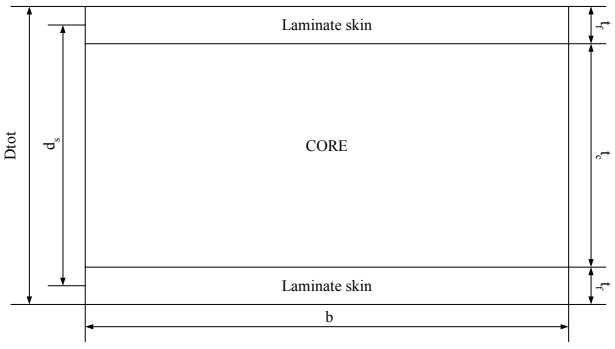

(c) Monocoque FRP sandwich beam model

Fig. 1

2. Adopted approach

For the comparative study, it is assumed that the flat-bar stiffened aluminium plate, the hat-section stiffened FRP single skin plates and the monocoque FRP sandwich plates to be composed of a series of beams. This implies that these beam models can be analysed using conventional statistically determinant and SQP optimisation approaches and their results can be extrapolated to learn lessons for the proposed stiffened plates. Fig. 1 shows the beam models, and L, a and b are 2.4m, 0.05m and 0.24m respectively. Three mechanical criteria are proposed and they are (1) space or volume equivalence, which translates to a limiting depth of a stiffener or sandwich beam

Table 1 Design variants for the beam models

Design Variants	Technical Constraint	Functional Constraints
Aluminium (6082), GFRP hat-section single skin, GFRP monocoque sandwich	Stress limit: 80, 100, 120, 140MPa.	Depth of stiffener constraint
	Deflection limit: L/150, L/200, L/250, L/300(mm)	Depth of stiffener constraint
Aluminium (6082), GFRP hat-section single skin, GFRP monocoque sandwich	Stress limit: 80, 100, 120, 140MPa. Deflection limit: L/150, L/200, L/250, L/300(mm)	A combination of stress and deflection limits for estimating plating thickness and stiffener depth
Various CFRP & GFRP hat-section single skin and monocoque sandwich	Stress limit: 80, 100, 120, 140MPa.	Depth of stiffener constraint
	Deflection limit: L/150, L/200, L/250, L/300(mm)	Depth of stiffener constraint
Various CFRP & GFRP hat-section single skin and monocoque sandwich	Stress limit: 80, 100, 120, 140MPa. Deflection limit: L/150, L/200, L/250, L/300(mm)	A combination of stress and deflection limits for estimating plating thickness and stiffener depth

Table 2 Material properties of the beam models

	E (Elastic modulus)	ρ (Material densities)
Aluminium 6082	72,000MPa	2640kg/m^3
Low modulus GFRP	13,800MPa	1540kg/m^3
High modulus GFRP	30,000MPa	1800kg/m^3
High strength CFRP	140,000MPa	1600kg/m^3
Ultra-high modulus CFRP	300,000MPa	1700kg/m^3
Hat-section stiffener former	Non-structural member	20kg/m^3
PVC foam core	22MPa (shear)	80kg/m^3

model: (2) strength equivalence, which translates to the ability to withstand a particular lateral pressure load; and (3) stiffness equivalence, which translates to the ability to be within a certain deflection (see, Table 1). The design metrics from this beam modelling would be the thickness of the plating, depth of stiffener/sandwich core and weight. Table 2 shows the materials properties of aluminium, CFRP and GFRP used in the beam models.

It is assumed that FRP laminates are monolithic; hence only a thickness value is calculated and no attempt is made to ascribe this in terms of ply details, make-up, fibre volume fractions etc. This can be taken up at a later stage when gross decisions about the choice of a particular configuration and material are made. For the flat-bar stiffened aluminium and the hat-section stiffened C/GFRP single skin beam models, the following bending stress and deflection equations are used.

$$\sigma_{\max} = \frac{qL^2 y}{8I} \tag{1}$$

$$\delta_{\max} = \frac{5qL^4}{384EI} \tag{2}$$

In the derivation of C and I for the hat-section stiffened configuration, geometric values from industry are referenced to obtain thickness relations among t_f, t_a and e. Thus, it is assumed that $t_f = 3 \times t_a$ and $t_a = e$.

For the monocoque sandwich beam model, it is assumed that the top and the bottom laminate skins have the same thickness and therefore only bending deflection term is considered in the derivation of the following stress equation (Zenkert, 1997; Deflection equation for this model is the same as Eq. (2)).

$$\sigma_{\max} = \frac{M}{EI}\frac{(t_f + t_c)}{2}E_f \tag{3}$$

In all above beam models, an applied lateral pressure load, q, is derived using the ABS rules (American Bureau of Shipping, 2003). The lateral pressure load of 3.3N/mm is obtained because the exemplified flat-bar stiffened aluminium plate is extracted from the superstructure of a marine vessel having 42.8m of waterline length.

3. Results from the beam modelling using the conventional statistically determinant approach

3.1 Results when depth is constrained

Fig. 2.(a)~(c) show the variation of weights with varying levels of stiffness or strength constraints for the stiffened aluminium, the hat-section stiffened GFRP single skin and the monocoque GFRP sandwich beam models. Consider the designs based on the strength constraint-these are green bars. Firstly, as the strength limit is raised, the weight of the beam models is reduced. However, the reduction is less steep in the GFRP single skin and sandwich beam models. Secondly, the hat-section stiffened GFRP single skin beam model emerges as the most weight efficient design. Next consider the designs based on the stiffness constraint-these are blue bars. As the stiffness limit is increased and the beam models are allowed to be more flexible, the weight of the beam models reduces. It is evident that the aluminium based design is more weight efficient than the GFRP based designs. Comparing the relative efficiencies of strength versus stiffness constraints in determining weights, it is apparent that a lighter aluminium design can be obtained in deflection-limited case, while a lighter GFRP design can be achieved in stress-limited case.

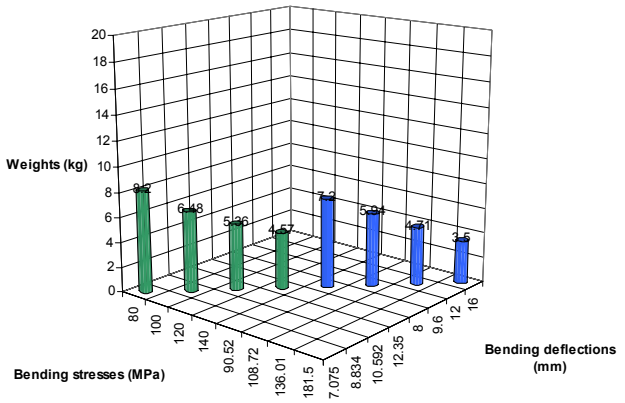

(a) Weights of the stiffened aluminium beam model

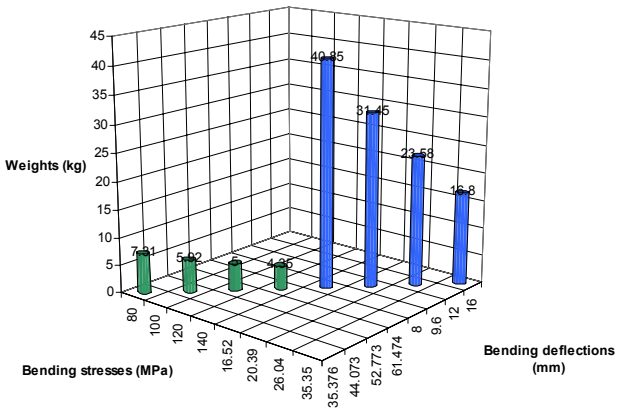

(b) Weights of the hat-section stiffened GFRP single skin beam model(E=13.8GPa)

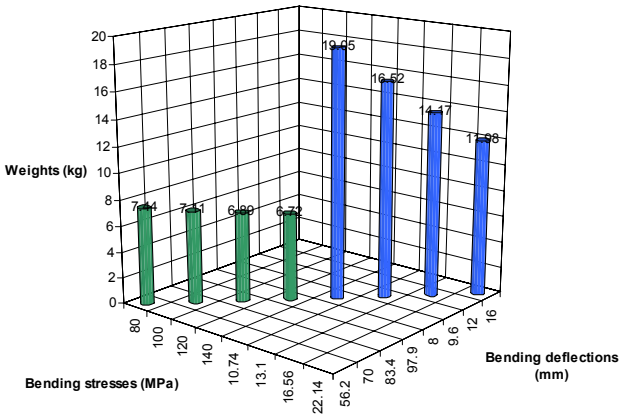

(c) Weights of the monocoque GFRP sandwich beam model(E_f=13.8GPa)

Fig. 2

Fig. 3.(a)~(f) show the variation of weights for the hat-section stiffened single skin and the monocoque sandwich configurations with the laminate skins being composed of high modulus GFRP (30GPa), ultra-high modulus CFRP (300GPa) and high strength CFRP (140GPa). Examine the strength based designs; it is clear that the use of higher stiffness laminates has a marginal effect in weight saving for the hat-section stiffened cases, see Fig. 3. (a)~(c). At a stress limit of 80MPa, the weight of the GFRP is 8.46kg and those of the high strength CFRP and the ultra-high modulus CFRP are 7.58kg and 8.02kg respectively. A similar trend of marginal influence on weight is noticeable for the sandwich configuration as well: the weight of the GFRP is 7.74kg and those of the high strength CFRP and the ultra-high modulus CFRP are 7.51kg and 7.63kg respectively (see Fig. 3.(d)~(f)). Now examine the stiffness based designs, the weight of the hat-section stiffened single skin configuration is significantly reduced as stiffness increases. At a deflection limit of L/300, the weight of the GFRP is 17.8kg as compared to 3.52kg and 2.01kg for the high strength and the ultra-high modulus CFRP. A similar reducing shift is noticed in the sandwich configuration

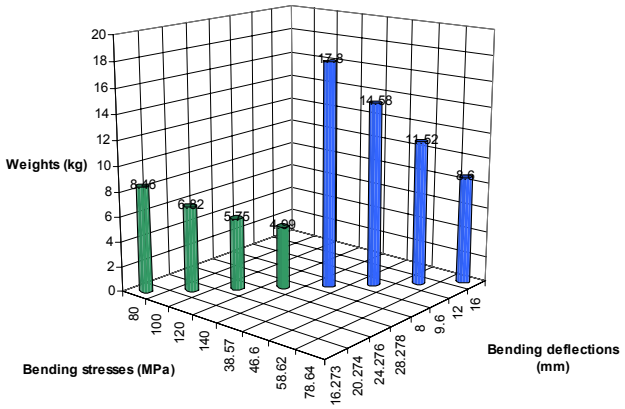

(a) Weights of the hat-section stiffened GFRP single skin beam model(E=30.0GPa)

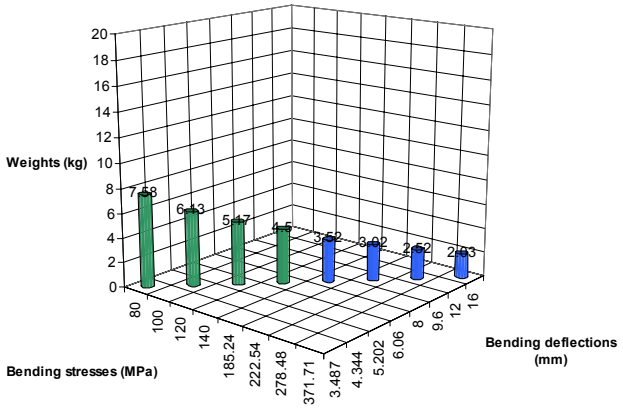

(b) Weights of the hat-section stiffened CFRP single skin beam model(E=140.0GPa)

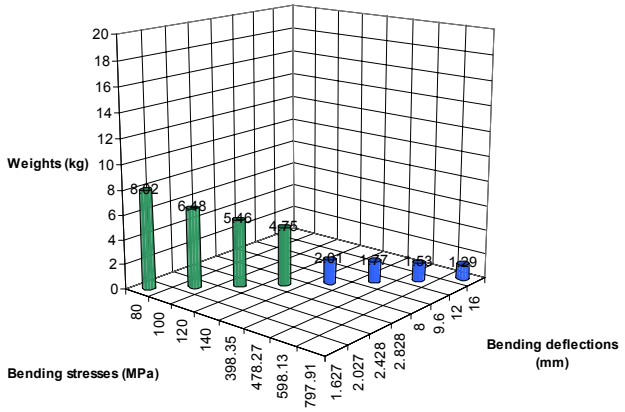

(c) Weights of the hat-section stiffened CFRP single skin beam model(E=300.0GPa)

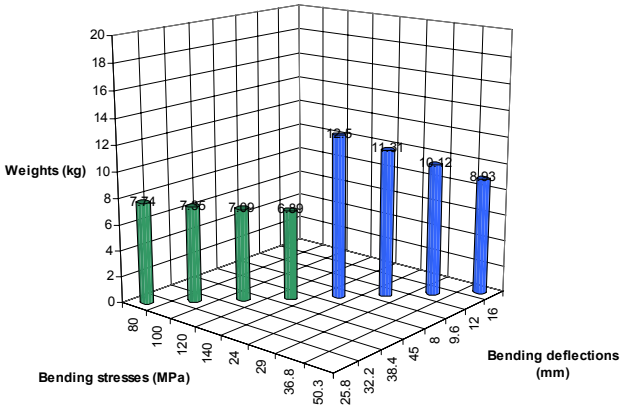

(d) Weights of the monocoque GFRP sandwich beam model(E_f=30.0GPa)

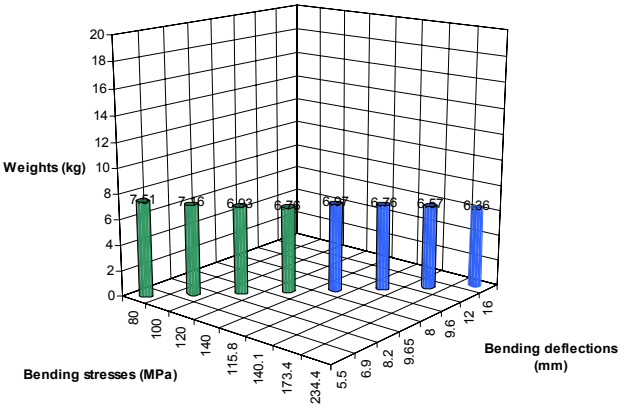

(e) Weights of the monocoque CFRP sandwich beam model(E_f=140.0GPa)

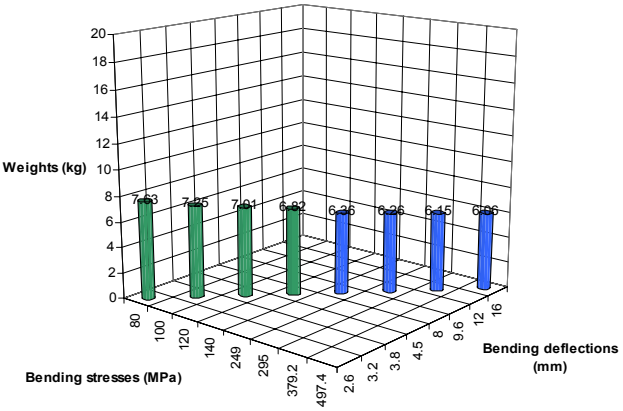

(f) Weights of the monocoque CFRP sandwich beam model(E_f=300.0GPa)

Fig. 3

as well; weight values for the GFRP, the high strength and the ultra-high modulus CFRP being about 12.5kg, 6.97kg and 6.36kg respectively. If a comparison is made between aluminium and high strength CFRP for the strength limited case (i.e. a stress limit of 80MPa), it can be noticed that the weight of the aluminium beam model is 8.2kg as compared to 7.58kg for the hat-section stiffened beam model and 7.51kg for the sandwich configuration. This implies 9.2% weight saving by adopting CFRP sandwich configuration. If a comparison is made between aluminium and ultra-high modulus CFRP for

the stiffness limited case (i.e. a deflection limit of L/300), it can be seen that the weight of the aluminium beam model is about 7.2kg as compared to 2.01kg for the hat-section stiffened configuration and 6.36kg for the sandwich configuration.

This implies a 258% weight saving by using the CFRP hat-section stiffened configuration.

3.2 Results when depth is unconstrained

Fig. 4. (a)~(c) show the three surfaces of weight as functions of stress and deflection for the aluminium beam model, the hat-section stiffened GFRP single skin beam model and the monocoque GFRP sandwich beam model. The figures show some interesting trends as follows,

- In general, the GFRP hat-section stiffened design is the most weight efficient, followed by the aluminium and the sandwich beam models.
- The GFRP hat-section stiffened beam model surface shows a distinctive flat nature, signifying that the effect of the given stress and deflection constraints is minimal.
- Sandwich configuration emerges as being markedly heavier, indicating that its stiffness and/or strength capabilities are not being utilised to the fullest under the given design constraints.

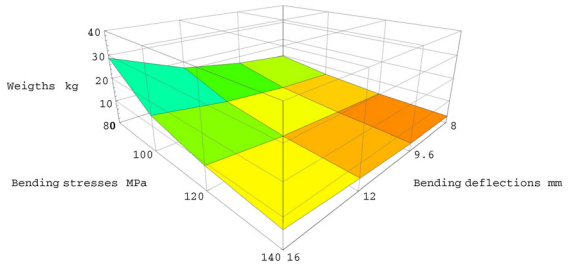

(a) Weight surface of the stiffened aluminium beam model

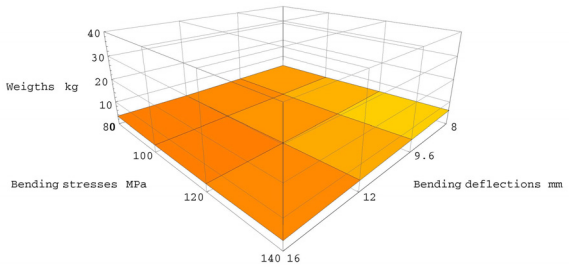

(b) Weight surface of the hat-section stiffened GFRP single skin beam model (E=13.8GPa)

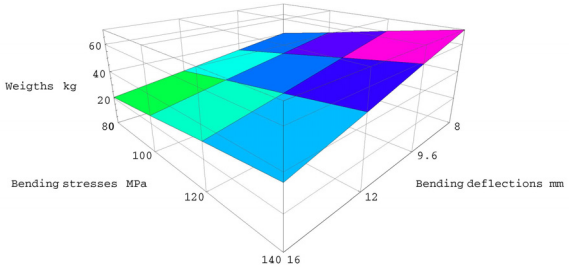

(c) Weight surface of the monocoque GFRP sandwich beam model (E_f=13.8GPa)

Fig. 4

In the context of the design constraints, it must be emphasised that some of their values may be unrealistic in practice. For example, it is likely that aluminium structures will experience stability limits lower than 140MPa.

Fig. 5(a)~(f) show the influence of using high modulus GFRP and ultra-high modulus and high strength CFRP laminate skins. Interesting trends from these figures are withdrawn as follows,

- The hat-section stiffened single skin configuration emerges to be more effective and weight efficient than the sandwich configuration when the GFRP laminate skins are used. However, this result changes as the laminate skins are made from the CFRP: the sandwich configuration emerges to be more effective and weight efficient.
- Changing low modulus GFRP into high modulus GFRP results in 'nearly the same' design for the hat-section stiffened single skin configuration and 'better' design for the sandwich configuration.
- For the hat-section stiffened single skin configuration, the use of the CFRP laminates does not provide weight saving option, while the sandwich configuration reduces its weight by having the CFRP laminate skins.
- In case of the hat-section stiffened single skin configuration, weight increases with increasing strength limits for the low modulus GFRP laminates and weight decreases with increasing strength limits for the high modulus GFRP, the ultra-high modulus and the high strength CFRP laminates.
- In case of the sandwich configuration, weight

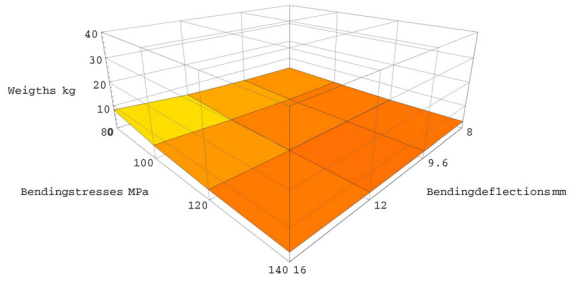

(a) Weight surface of the hat-section stiffened GFRP single skin beam model (E=30.0GPa)

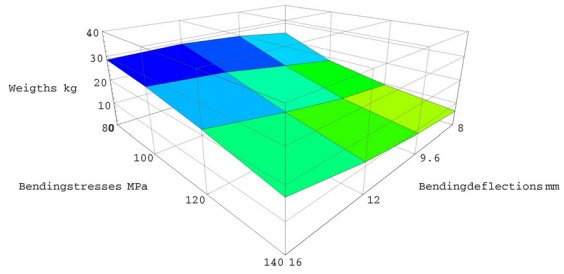

(b) Weight surface of the hat-section stiffened CFRP single skin beam model (E=140.0GPa)

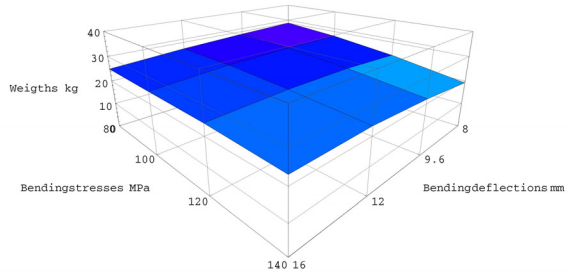

(c) Weight surface of the hat-section stiffened CFRP single skin beam model (E=300.0GPa)

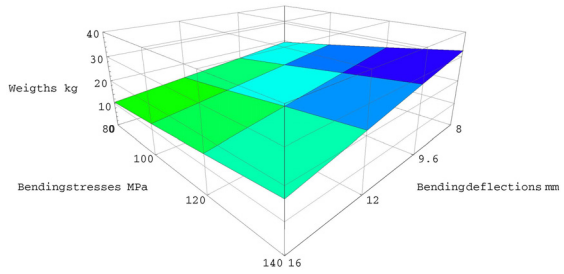

(d) Weight surface of the monocoque GFRP sandwich beam model (E_f=30.0GPa)

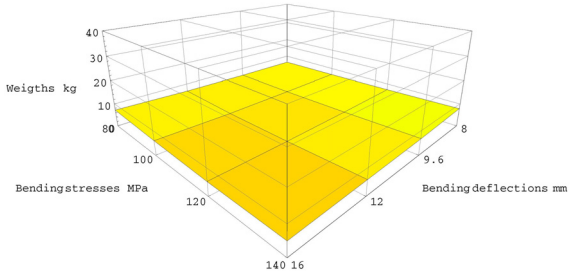

(e) Weight surface of the monocoque CFRP sandwich beam model (E_f=140.0GPa)

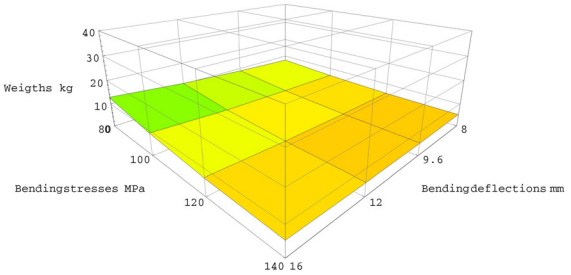

(f) Weight surface of the monocoque CFRP sandwich beam model (E_f=300.0GPa)

Fig. 5

increases with increasing strength limits for the laminate skins having the GFRP and weight decreases with increasing strength limits for the CFRP laminate skins.

4. Results from the beam modelling using the SQP optimisation approach

From the comparative study of the hat-section stiffened single skin and sandwich beam models using the elastic closed-form solutions in conjunction with equality stress and deflection limits, impractical flange and laminate skin thicknesses and total depth are obtained for some structural topologies, see Table 3. In Table 3, √ denotes acceptable scantlings while × denotes impractical scantlings. This judgement is made by knowing minimum and maximum structural thickness in a practical sense. In that decision, E-glass woven roving having a weight of 566g/m^2 with epoxy resin and vacuum assisted resin infusion as a manufacturing method for a laminate of 0.9m^2 area is referenced. It should be mentioned that this referencing is approximation as the structural topologies varied from low modulus GFRP to ultra-high modulus CFRP.

From Table 3, it can be thought that the impractical thicknesses of some structural topologies are calculated due to the use of the strength and stiffness equality constraints. Thus the idea of adopting the strength and stiffness inequality constraints is introduced with a

Table 3 Calculated scantlings of the FRP beam models and their practicality

Structural topology	Modelling	t_f	E	t_a	D_{tot}	Practicality
Hat-section stiffened single skin configuration	M-1/5/8	2.8~5.0	0.9~1.7	0.9~1.7	125	√
	M-1/6/8	12.3~32.7	4.1~10.9	4.1~10.9	125	×
	M-2/5/8	2.8~5.0	0.9~1.7	0.9~1.7	125	√
	M-2/6/8	5.1~11.1	1.7~3.7	1.7~3.7	125	√
	M-3/5/8	2.8~5.0	0.9~1.7	0.9~1.7	125	√
	M-3/6/8	1.0~2.1	0.3~0.7	0.3~0.7	125	×
	M-4/5/8	2.8~5.0	0.9~1.7	0.9~1.7	125	√
	M-4/6/8	0.5~1.0	0.2~0.3	0.2~0.3	125	×
	M-1/7/9	0.1~1.1	0.02~0.4	0.02~0.4	309~1324	×
	M-2/7/9	0.2~5.0	0.1~1.6	0.1~1.6	127~541	×
	M-3/7/9	4.6~28.8	1.6~9.6	1.6~9.6	37~93	√
	M-4/7/9	16.5~28.6	5.5~9.5	5.5~9.5	22~47	√
Structural topology	Modelling	T_f (top skin)	T_f (bottom skin)	t_c	D_{tot}	Practicality
Monocoque sandwich configuration	M-1/5/8	0.6~1.0	0.6~1.0	123~123.8	125	√
	M-1/6/8	3.7~7.9	3.7~7.9	109~117.6	125	√
	M-2/5/8	0.6~1.0	0.6~1.0	123~123.9	125	√
	M-2/6/8	1.6~3.4	1.6~3.4	118~121.8	125	√
	M-3/5/8	0.6~1.0	0.6~1.0	123~123.9	125	√
	M-3/6/8	0.3~0.7	0.3~0.7	123.6~124	125	×
	M-4/5/8	0.6~1.0	0.6~1.0	123~123.9	125	√
	M-4/6/8	0.2~0.3	0.2~0.3	124~124.7	125	×
	M-1/7/9	0.001~0.2	0.001~0.2	463~1579	463~1579	×
	M-2/7/9	0.001~0.5	0.001~0.5	227~756	228~756	×
	M-3/7/9	0.3~1.8	0.3~1.8	68~205.9	72~206.6	×
	M-4/7/9	0.6~2.8	0.6~2.8	44~125.6	50~126.7	√

view to minimise weight using a suitable optimisation tool. Here, the SQP algorithm (Gill *et al.*, 1981) for a nonlinear inequality constrained problem with bounds is adopted.

Where, M-1: low modulus GFRP/M-2: high modulus GFRP/M-3: high strength CFRP/M-4: ultra-high modulus CFRP/M-5: Strength constraint/M-6: Stiffness constraint/M-7: Strength and stiffness constraints/ M-8: Depth of stiffener constraint/M-9: Free depth of stiffener

In this method, an approximation is made of the Hessian of the Lagrangian function using a quasi-Newton updating algorithm at each major iteration. This is then used to generate a Quadratic Programming (QP) subproblem and its solution is used to form a search direction for a line search procedure. In general, the problem can be depicted as follows,

$$\min f(x) \tag{4}$$

subject to

$$\begin{aligned} &h_i(x) = 0, \quad i = 1,...,m_e \\ &h_i(x) =\leq 0, \quad i = m_e + 1,...,m \\ &x_L \leq x \leq x_U \end{aligned} \tag{5}$$

Where x is the vector of design variables, ($x \in \Re^n$), $f(x)$ is the objective function that returns a scalar value ($f(x): \Re^n \rightarrow \Re$), and the vector function $h(x)$ returns the values of the equality and inequality constraints evaluated at x ($h(x): \Re^n \rightarrow \Re^m$). In summary, Fig. 6 shows the flowchart of the SQP method with line search.

For calculating the weight of the beam models, the following equations are considered as object functions,

For the hat-section stiffened single skin beam model:

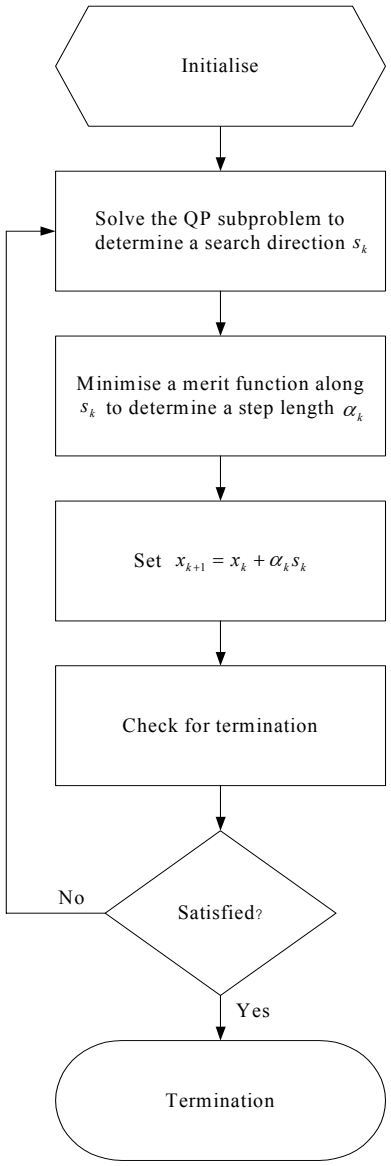

Fig. 6 SQP method with line search

Minimise

$$f(x) = (t_f \times b \times L \times \rho_{laminate} \times 10^{-9}) + (2 \times 1.4 \times e \times d_t \times L \times \rho_{laminate} \times 10^{-9}) + ((\frac{t_a \times (a+c)}{2}) \times L \times \rho_{laminate} \times 10^{-9}) + (\frac{d_t \times ((b-2\times a-2\times 1.4\times e)+(c-(2\times 1.4\times e)))}{2} \times L \times \rho_{former} \times 10^{-9}) \quad (6)$$

Subject to,

$\frac{qL^2 y}{8I} \le \sigma_{\max}$, $\frac{5qL^4}{384EI} \le \delta_{\max}$, $1\text{mm} \le t_a \le 10\text{mm}$ and $50\text{mm} \le Dtot \le 300\text{mm}$.

For the monocoque sandwich beam model:

Minimise

$$f(x) = 2 \times (b \times L \times t_f \times \rho_{laminate} \times 10^{-9}) + (b \times L \times (Dtot - 2t_f) \times \rho_{core} \times 10^{-9}) \quad (7)$$

Subject to,

$\frac{wL^2}{8bt_f(Dtot - t_f)} \le \sigma_{\max}$, $\frac{5}{192}\frac{wL^4}{E_f bt_f (t_f - Dtot)^2} \le \delta_{\max}$,

$1\text{mm} \le t_f \le 10\text{mm}$ and $50\text{mm} \le Dtot \le 350\text{mm}$

The results are shown in Fig. 7.(a)~(h).

From the above figures the following observations can be withdrawn:

- Compared to the design procedures based on the conventional statistically determinant approach employing equality constraints, the present optimisation based design procedure produces the flange and laminate skin thicknesses and total depth of the hat-section stiffened single skin and sandwich beam models close to practice.
- Switching from the GFRP to the CFRP materials results in much lighter sandwich configurations, while this material change produces only marginal weight saving for the hat-section stiffened single skin configurations. This implies that the use of higher specific modulus (E/ρ) materials in sandwich concept is a benefit.
- It is interesting to note that when the hat-section stiffened single skin and sandwich beam models have the GFRP laminates, changes in geometry dimensions are only made when the stiffness limits are changed. However, this finding is not true for both beam models when they have the CFRP laminates: the results show variability within the same stiffness limit, although they are not widely varied. From these findings, it may be said that stiffness limit is the design limitation for flexible laminates, and the strength limit is the design limitation for stiff laminates.
- It can easily be noticed that good weight saving is achieved from the optimisation based design

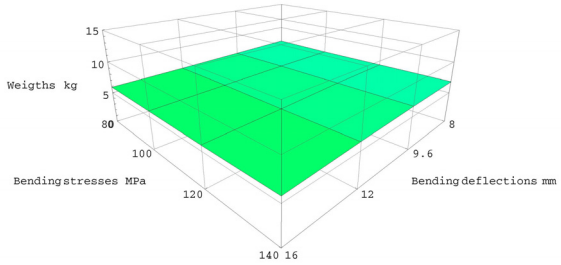

(a) Weight surface of the hat-section stiffened GFRP single skin beam model (E=13.8GPa)

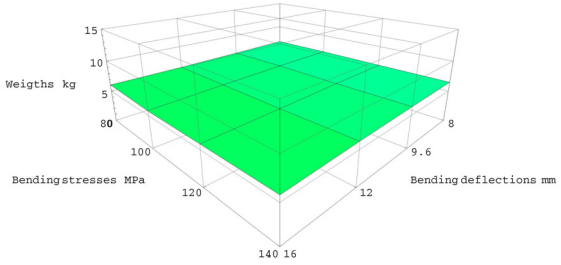

(b) Weight surface of the hat-section stiffened GFRP single skin beam model (E=30.0GPa)

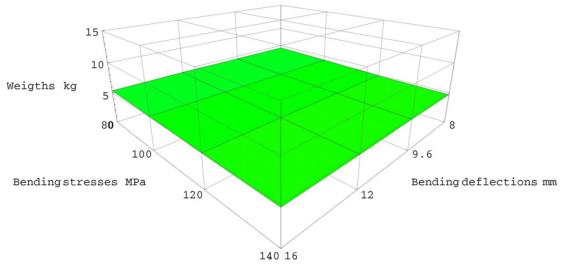

(c) Weight surface of the hat-section stiffened CFRP single skin beam model (E=140.0GPa)

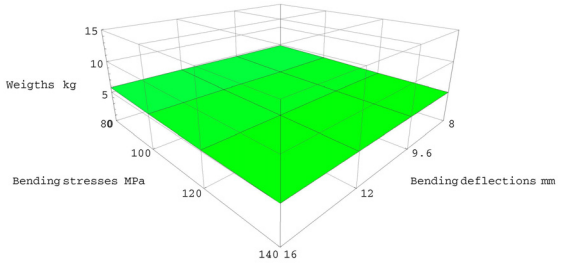

(d) Weight surface of the hat-section stiffened CFRP single skin beam model (E=300.0GPa)

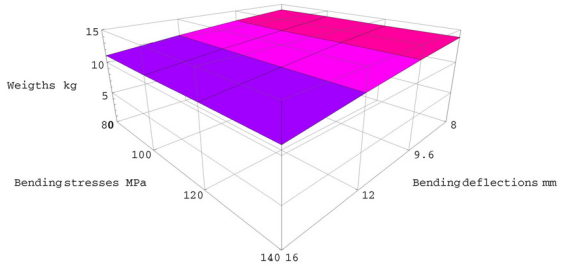

(e) Weight surface of the monocoque GFRP sandwich beam model (E_f=13.8GPa)

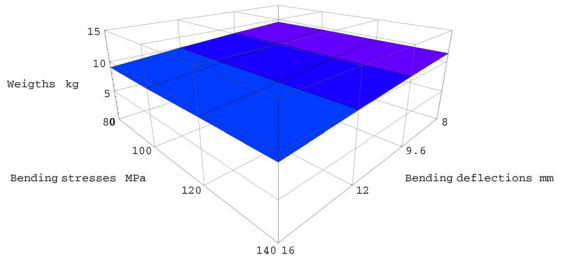

(f) Weight surface of the monocoque GFRP sandwich beam model (E_f=30.0GPa)

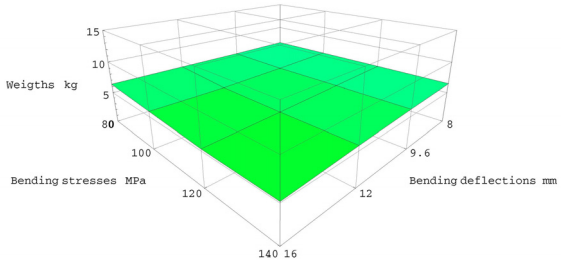

(g) Weight surface of the monocoque CFRP sandwich beam model (E_f=140.0GPa)

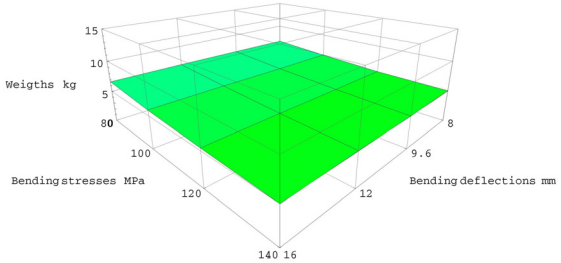

(h) Weight surface of the monocoque CFRP sandwich beam model (E_f=300.0GPa)

Fig. 7

procedure. This weight saving is due to the strength and stiffness inequality constraints in conjunction with the imposed bounds.

5. Discussions

In carrying out the comparative study, two levels of analyses are conducted: (1) a statistically determinate structural analysis incorporating the strength and stiffness equality constraints; and (2) a structural optimisation analysis based on the strength and stiffness inequality constraints with bounds. In both (1) and (2) analyses, the weights of the structural alternatives are one of primary outcomes along with

Table 4 Maximum weight comparison based on the conventional statistically determinate approach

Maximum weights		Aluminium alloy 6082 (AA)		
		Depth of stiffener constraint		Free depth of stiffener
		Strength limits	Stiffness limits	Strength & stiffness limits
Hat-section stiffened single skin plate	Low modulus GFRP	HSS 〈* AA	HSS 〉@ AA	HSS 〈@ AA
	High modulus GFRP	HSS 〉* AA	HSS 〉@ AA	HSS 〈@ AA
	High strength CFRP	HSS 〈* AA	HSS 〈# AA	HSS 〉* AA
	U-H modulus CFRP	HSS 〈* AA	HSS 〈@ AA	HSS 〉* AA
Monocoque sandwich plate	Low modulus GFRP	MS 〈* AA	MS 〉@ AA	MS 〉@ AA
	High modulus GFRP	MS 〈* AA	MS 〉* AA	MS 〉* AA
	High strength CFRP	MS 〈* AA	MS 〈* AA	MS 〈@ AA
	U-H modulus CFRP	MS 〈* AA	MS 〈* AA	MS 〈@ AA

*Marginal weight saving
Between marginal and good weight savings
@ Good weight saving

Table 5 Maximum weight comparison based on the optimisation approach

Maximum weights		Aluminium alloy 6082 (AA)
		Free depth of stiffener
		Strength & stiffness limits with lower/ upper bounds
Hat-section stiffened single skin plate	Low modulus GFRP	HSS 〈@ AA
	High modulus GFRP	HSS 〈@ AA
	High strength CFRP	HSS 〈@ AA
	U-H modulus CFRP	HSS 〈@ AA
Monocoque sandwich plate	Low modulus GFRP	MS 〈@ AA
	High modulus GFRP	MS 〈@ AA
	High strength CFRP	MS 〈@ AA
	U-H modulus CFRP	MS 〈@ AA

@ Good weight saving

the geometry dimensions and their comparison is shown in Tables 4 and 5 (It should be mentioned that the results shown in these tables are based on the maximum weights per each modelling case shown in Table 3).

When the design constraints of strength and stiffness equality are imposed, the use of the FRP composites materials in the place of metallic structures is found favourable. Especially it is encouraged to use the CFRP materials, although, the CFRP hat-section single skin configuration is slightly heavier than the aluminium model under the free depth of stiffener constraint, see Table 4 (it is judged that the given stress and deflection limits with the hat-section stiffened single skin configuration are not recommended). Additionally, when the design constraints of strength and stiffness inequality are used in conjunction with the optimisation method, the weights of the FRP composites material based models are reduced compared to the results shown in Table 4. Of course, the weight of the aluminium based design used for the comparison in Table 5 is obtained from the conventional statistically determinant approach but it clearly demonstrates the benefit of using the optimisation technique to the current structural design procedure and the results are satisfied within the imposed design constraints.

6. Conclusions

Structural design aspects arising from the use of the FRP composites materials into structures previously built in metallic materials are examined in this paper. To look those aspects over, the conventional statistically determinant and SQP optimisation approaches are used in conjunction with the design constraints such as space, strength and stiffness equivalence for the stiffened plates. Construction materials of the stiffened plates are varied as 6082 aluminium alloy, low and high moduli GFRP, high strength and ultra-high modulus CFRP. Structural topology of these stiffened plate is altered such as the flat-bar stiffened plate, the hat-section stiffened single skin plate and the monocoque sandwich plate. Through the comparative study, useful information for marine structural designers, especially at the preliminary design stage, is derived

by recommending efficient structural configurations and building materials for the stiffened plate in marine vessels.

Acknowledgement

This research work was supported by Ministry of Knowledge and Economy, Korea through the Industrial Strategic Technology Development Program (Grant No. 10033791) and also supported by research funds of Kunsan National University. The author would like to thank their supports.

References

American Bureau of Shipping (2003) Guide for Building and Classing, High-Speed Naval Craft (Part 3: Hull Construction and Equipment, Chapter 2: Hull Construction, Section 2: Design Pressure).

Clarkson, J. (1965) The Elastic Analysis of Flat Grillages: With Particular Reference to Ship Structures, The Syndics of the Cambridge University Press.

Davalos, J.F., Qiao, P., Barbero, E.J. (1996) Multiobjective Material Architecture Optimization of Pultruded FRP I-beams, *Composite Structures*, 35, pp.271~281.

Gill, P.E., Murray, W., Wright, M.H. (1981) Practical Optimisation, Academic Press, London.

He, Y., Aref, A.J. (2003) An Optimization Design Procedure for Fiber Reinforced Polymer Web-core Sandwich Bridge Deck Systems, *Composite Structures*, 60, pp.183~195.

Liu, J.S., Hollaway, L. (2000) Design Optimisation of Composite Panel Structures with Stiffening Ribs under Multiple Loading Cases, *Computers and Structures*, 78, pp.637~647.

Muckle, W. (1967) Strength of Ships' Structures, Edward Arnold (Publishers) Ltd., London.

Sedaghati, R., Esmailzadeh, E. (2003) Optimum Design of Structures with Stress and Displacement Constraints using the Force Method, *International Journal of Mechanical Sciences*, 45, pp.1369~1389.

Smith, C.S. (1990) Design of Marine Structures in Composite Materials, Elsevier Science Publishers Ltd.

Zenkert, D. (1997) An Introduction to Sandwich Construction, EMAS, Chameleon Press Ltd., London.

Nomenclature

a	Hat-section stiffener crown width and flat bar stiffener flange width
b	Effective width of plating associated with stiffeners
c	Expanded hat-section stiffener crown width
c_{al}	Thickness of flat bar stiffener web
d	Depth of flat bar stiffener web
d_t	Depth of former in hat-section stiffened single skin structure
D_{tot}	Total depth of structure
e	Thickness of hat-section stiffener web
e_{al}	Thickness of stiffened aluminium structure base
E	Elastic modulus
E_f	Elastic modulus of laminate skin
f	Thickness of flat bar stiffener flange
$f(x)$	Objective function
$h(x)$	Vector function
I	Second moment of the area
L	Length of structure
M	Bending moment
q	Design pressure load
s_k	Search direction vector at kth iteration
t_a	Thickness of hat-section stiffener crown
t_c	Thickness of core
t_f	Thickness of laminate skin and hat-section stiffened single skin structure base
w	Deflection
x	Vector of design variables
$x_{k/k+1}$	k / k+1th iteration design variables
x_L	Lower bound on x
x_U	Upper bound on x
y	Distance from the neutral axis to the point where maximum stress occurs
α_k	kth iteration step length in line search
ρ	Material densities

● 논문접수일 2010년 11월 3일
● 논문심사일 2010년 11월 4일
● 게재확정일 2010년 11월 25일